

---

# Learning from Small Data Through Sampling an Implicit Conditional Generative Latent Optimization Model

---

Idan Azuri<sup>1</sup> Daphna Weinshall<sup>1</sup>

## Abstract

We revisit the long-standing problem of *learning from small sample*. In recent years major efforts have been invested into the generation of new samples from a small set of training data points. Some use classical transformations, others synthesize new examples. Our approach belongs to the second one. We propose a new model based on conditional Generative Latent Optimization (cGLO). Our model learns to synthesize completely new samples for every class just by interpolating between samples in the latent space. The proposed method samples the learned latent space using spherical interpolations (*slerp*) and generates a new sample using the trained generator. Our empirical results show that the new sampled set is diverse enough, leading to improvement in image classification in comparison to the state of the art, when trained on small samples of CIFAR-100 and CUB-200.

## 1. Introduction

Modern deep Convolutional Neural Networks (CNNs) define the state of the art in image classification, as well as many other problems in a wide range of applications. Typically enormous amounts of labeled data are used to train the networks. It is not obvious whether this success can be replicated in domains where the resource of labeled data is not widely available. While hardly unexplored, the question of learning from a small sample remains a very important and challenging problem, not least so in the context of deep learning and image classification. The differences (sometimes subtle) between the general problem of learning from small sample, and the related problems of few-shot learning and learning from imbalanced datasets, are briefly discussed in the next section.

<sup>1</sup>The Hebrew University of Jerusalem. Correspondence to: Idan Azuri <idan.azuri@cs.huji.ac.il>, Daphna Weinshall <daphna@cs.huji.ac.il>.

Different approaches have been explored to address this problem, as reviewed in the next section. The problem can be alleviated by imposing a strong prior on the model, which is less relevant in the context of deep learning, and by employing regularization. Data augmentation may help, reflecting the availability of some prior knowledge about the data. Methods employing semi-supervised (Odena, 2016) and transductive learning (Vapnik, 1998) make use of unlabeled data, when available. Self training approaches can also boost performance when labels are scarce. Finally, one may compute a generative model from the training data, and use it to generate new samples. This is the approach we explore in this paper. Clearly, the different approaches are not mutually exclusive and can be used jointly to further boost performance.

Using generative models to augment the training sample is very appealing, especially at present time when very powerful deep generative models are becoming available. The problem is that in general, these models require a very large (possibly unlabeled) sample in order to achieve effective training, and therefore can only be used to augment the training set in the semi-supervised scenario. To avoid this difficulty, our method leverages a recent generative model - GLO (Bojanowski et al., 2018), which can be trained effectively from a small sample. This generative method has been shown to be as effective as adversarial models for image reconstruction, though it is not as effective for the generation of realistic looking new images.

More specifically, the architecture we propose is based on the GLO model described in Section 3.2. GLO learns a latent space code for each data point separately. In order to improve the properties of the latent space, pushing examples from the same class to lie close to each other and as much as possible separated from the remaining points, we add a classifier to the basic architecture, which is trained using the known multi-class labels of the data. We note that training is not adversarial, and therefore this classifier is not equivalent to the discriminator in the GAN (Generative Adversarial Network) architecture. Additional modifications include the concatenation of noise to the latent space vector. The full model is described in Section 3.

The modified architecture allows us to effectively sample

specific areas in the latent space and synthesize novel images as explained in Section 3.2. In this way our method bears some similarity to (Chawla et al., 2002), a method designed to deal with the problem of imbalanced datasets by creating synthetic minority class examples. The empirical evaluation described in Section 4 shows the success of our model in improving classification performance while training with a small sample, especially in the extreme conditions where the sample size is very small indeed.

The rest of the paper is organized as follows. In Section 3 we describe cGLO, a new method for data synthesis which can be effectively trained from a small number of labeled points from each class. Our method can make use of unlabeled data when available, further benefiting from additional data in the semi-supervised and transductive learning scenarios. In Section 4 we describe how synthetic images are used to boost the training of a discriminative deep classifier. In Section 5 we demonstrate the superior performance of our method when compared to alternative methods under extreme low sample conditions. We provide an ablation study and further investigate alternative design choices and their effect on classification performance.

## 2. Related Work

Two decades ago, the problem of learning from a small sample received considerable attention mainly in the context of Bayesian inference, see for example (Baxter, 1997; Thrun & Pratt, 1998; Fei-Fei et al., 2004). Bayesian methods rely on the existence of a large dataset which is correlated with the test set. Under this assumption, a prior can be established and used to identify test examples from unseen classes. These methods have been revisited in recent years and largely investigated in the context of *few-shot learning* or *k-shot learning*. In a commonly used setup of *few-shot learning*, at train time there are many classes with many labeled examples from each class. At test time, some novel classes (usually 5) with only a few examples per class are given, alongside query images from the same novel classes. In contrast, our method is not based on transfer learning, but when additional transfer data is available, it may benefit from working in conjunction with a method that does.

A very useful and common technique to overcome the small sample problem is *data augmentation*, as discussed by Tanner & Wong (1987). This include augmentation in the image domain for image classification (e.g., Baird, 1993; Krizhevsky et al., 2012a; Cubuk et al., 2018), time-series transformations for natural language processing tasks (e.g., Kobayashi, 2018; Zhang et al., 2015), speech recognition (e.g. Park et al., 2019), and machine translation (e.g., Fadaee et al., 2017; Wang et al., 2018). In the following literature review we divide the prior work to two complementary directions: augmentation based on assumed invariance in the

data, and the generation of a new sample using generative models. Metric learning can also be used for this purpose (e.g., Hertz et al., 2006; Li et al., 2019), where recently Barz & Denzler (2019) showed that using the cosine distance may improve learning from small sample.

**Invariance-based augmentation.** Common augmentation techniques for image classifications include translating the image by a few pixels, adding Gaussian noise, and flipping the image horizontally or vertically. These techniques require prior knowledge on the data. For instance, vertical flip augmentation of the digit 6 will change its semantic meaning to 9. Methods such as AutoAugment (Cubuk et al., 2018), as well as Fast Augment (Lim et al., 2019; Hataya et al., 2019) and Smart Augmentations (Lemley et al., 2017), achieve further improvement by searching for the optimal set of augmentations in a predefined set of classical transformations, including random crop, flip, rotation, scale, and translation. The major drawback of such methods lies in the enormous space that needs to be searched, and the huge resources that are needed to perform an effective search.

Additional augmentation methods in image classification include *Cutout* (DeVries & Taylor, 2017b), which randomly masks a square region in an image at every training step and thus affects the nature of the learned features, and *Random Erasing* (Zhong et al., 2017), where similarly to dropout randomly chosen rectangular regions in the image have their pixels erased or replaced by random values. *MixUp* (Zhang et al., 2017) uses Alpha-blending of two images to form a new image, while regularizing the CNN to favor a simple linear behavior in between training images. *MixMatch* (Berthelot et al., 2019) augments MixUp by self training, generating guessed labels for each unlabeled example. We note that these methods are not always effective on very small datasets, and may even degrade classification performance as shown in Table 1.

**Data Augmentation with Generative models.** As alluded to above, generative models can be a powerful tool for data augmentation by making it possible under ideal conditions to sample totally new examples. Most of the methods which rely on generative models target the few-shot learning scenario. Among these methods, Delta-Encoder (Schwartz et al., 2018) investigates the use of a modified AutoEncoder: the model gets two examples from a known class and then learns the ‘delta’ between the two examples in order to generate new examples for novel classes. DAGAN (Antoniou et al., 2018) employs a GAN composed of a U-net generator and a DenseNet discriminator. Zhang et al. (2019) modified the discriminator of a semi-supervised GAN to return  $2N$  outputs, where the first  $N$  elements denote class probability, and the remaining  $N$  outputs denote the probability that the example is fake. Methods such as (DeVries & Taylor, 2017a;

Liu et al., 2018) also make use of Auto-Encoders. When using an Adversarial AutoEncoder (AAE), one can populate "dead zones" in the latent space by initializing it uniformly and then applying MixUp (Zhang et al., 2017). This method requires a large amount of (labeled or unlabeled) data in order to be effective.

All of these methods try to leverage generative models by sampling new synthetic examples from the learned distribution of the data. However, the estimation of the latent space for a given dataset is challenging and requires many training examples. In the low-shot case the estimated data distribution is less reliable, and it is therefore necessary to rely on the joint distribution of related classes. Thus one approach lets the learning model share its parameters across all classes, using the same generator in a GAN architecture, or the same encoder and decoder in an Auto-Encoder. In the small sample case, the few labeled examples do not represent the true data distribution very reliably, resulting in poor generalization and low quality synthetic data.

All in all, although GAN models have achieved tremendous success in generating realistic novel images (Brock et al., 2018; Karras et al., 2019), GAN based models have two major drawbacks that make them hard to use for data augmentation. The first is their sensitivity to hyperparameters when trying to reach the Nash equilibrium in the training process, and avoiding mode collapse. The second is the dependency on very large datasets (Goodfellow, 2017).

### 3. Our Model

We propose a method for multi-class image classification from small sample, which consists of data augmentation with a generative model. Specifically, in order to use modern deep learning classifiers, which typically require large amounts of training data, we augment the small training set by sampling from a generative model. Our generative model, called cGLO, is based on the GLO architecture (Bojanowski et al., 2018) which can be trained effectively from a small sample. This architecture is modified so that it can benefit from both labeled and unlabeled data. With access to only small amounts of unlabeled data or none at all, our results surpass the state of the art.

#### 3.1. Model Overview

The generative model we use to sample new data includes the basic GLO architecture with generator  $G_\theta$ , and an added small classifier  $f_\phi$  which is trained to classify the labeled data (see Fig. 1). Training is not adversarial, and therefore this classifier is nothing like the discriminator in the GAN (Generative Adversarial Network) architecture. As in (Bojanowski et al., 2018), the latent space is initialized randomly  $\{z_i \in Z\}$  where  $Z$  is the unit sphere in  $\mathbb{R}^d$ . Every

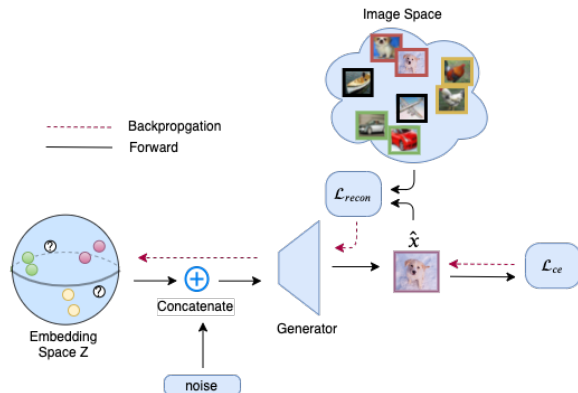


Figure 1. Schematic illustration of our method. Every  $z_i \in Z$ , where  $Z$  denotes the unit sphere, is mapped to a specific image  $x_i$  in the image space. In this illustration, the color of each image frame marks the class label of the image (pink:dog, green:cars, yellow:bird), while black frames mark unlabeled images. The classifier is used to propagate error only when a label is given.

vector  $z_i$  is mapped to an image  $\{x_i \in X | x_i \in \mathbb{R}^{3 \times H \times W}\}$  from the given (small) training set.

The training process has two modes: With unlabeled data, the reconstruction loss in (2) is used to train  $G_\theta$  just like the original GLO model. With labeled data, the reconstruction loss is augmented with the cross-entropy loss corresponding to the loss of the added classifier  $f_\phi$  (see Fig. 1).

Here we use the perceptual loss (Johnson et al., 2016) to measure the reconstruction loss. More specifically, in order to compute the perceptual loss we extract the activation vectors in layers  $conv_{1,2}$ ,  $conv_{2,2}$ ,  $conv_{3,2}$ ,  $conv_{4,2}$  and  $conv_{5,2}$  of a VGG-16 network. Denoting the output tensor of layer  $conv_{j,2}$  for input image  $x$  by  $\xi_j(x)$ , we compute the difference between the original image and its reconstructed version by:

$$\mathcal{L}_{percep}(x_i, z_i; \theta) = \sum_j \lambda_j \|\xi_j(G_\theta(z_i)) - \xi_j(x_i)\|_1 \quad (1)$$

Above  $\theta$  denotes the parameters of the generator  $G$ , and  $\lambda_j$  the weight of layer  $j$  (usually the weighted average).

#### 3.2. Generative Latent Optimization

Our method is described in Alg. 1. Its components are described next.

**Generative model.** Generative Latent Optimization (GLO) (Bojanowski et al., 2018) is a relatively simple method, relying on a relatively small number of parameters. GLO maps every image  $x_i$  from the dataset to a low-dimensional random vector  $z_i$  in the latent space  $Z$ . It then passes the random vector into a generator  $G_\theta(\cdot)$ , which

**Algorithm 1** cGLO. The algorithm optimizes the reconstruction loss  $\mathcal{L}_{percep}$  of generator  $G_\theta$ , and the cross entropy loss  $\mathcal{L}_{ce}$  of discriminator  $f_\phi$ .

**Input:** unlabeled data  $P_{D_u}$ , labeled data  $P_{D_L}$ ,  $\gamma$ , epochs  
epoch = 0

Initialize  $\{\mathbf{z}_i\}_{i=1}^n$  where  $\{\mathbf{z}_i \in Z : \|\mathbf{z}_i\|_2 = 1\}$

**repeat**

**for**  $(x_i, y_i) \in P_{D_L}$  **do**

$$\mathcal{L}_{percep} = \sum_j \lambda_j \|\xi_j(G_\theta(\mathbf{z}_i)) - \xi_j(x_i)\|_1$$

$$\mathcal{L}_{ce} = \mathcal{L}_{CE}(f_\phi(G_\theta(\mathbf{z}_i)), y_i)$$

$$\mathcal{L} = \mathcal{L}_{percep} + \gamma \mathcal{L}_{ce}$$

  Update  $\{\mathbf{z}_i\}, \theta, \phi$  using the gradient of  $\mathcal{L}$

**end for**

(this part is optional for transductive learning mode)

**for**  $x_i \in P_{D_u}$  **do**

$$\mathcal{L} = \sum_j \lambda_j \|\xi_j(G_\theta(\mathbf{z}_i)) - \xi_j(x_i)\|_1$$

  Update  $\{\mathbf{z}_i\}, \theta$  using the gradient of  $\mathcal{L}$

**end for**

  epoch + = 1

**until** epoch > epochs

is optimized to minimize the reconstruction loss between  $G_\theta(\mathbf{z}_i)$  and  $x_i$ .

Formally, let  $\{x_1, x_2, \dots, x_n\} \in X$  denote a set of images where  $x_i \in \mathbb{R}^{3 \times W \times H}$ . Choose  $n$   $d$ -dimensional random vectors on the unit sphere  $\{\mathbf{z}_1, \mathbf{z}_2, \dots, \mathbf{z}_n\} \in Z$  where  $Z \subseteq \mathbb{R}^d$ . Pair every image  $x_i \in X$  with a random vector  $\mathbf{z}_i \in Z$ , to achieve the mapping  $\{(x_1, \mathbf{z}_1), \dots, (x_n, \mathbf{z}_n)\}$ . Finally, learn jointly the parameters  $\theta$  of the generator  $G_\theta : Z \rightarrow X$ , where the optimal set  $\{\mathbf{z}_i\}$  and parameters  $\theta$  are obtained by minimizing the following objective:

$$\min_{\theta} \sum_{i=1}^n \left[ \min_{\mathbf{z}_i \in Z} \mathcal{L}_{percep}(x_i, \mathbf{z}_i; \theta) \right] \quad (2)$$

s.t.  $\|\mathbf{z}_i\|_2 = 1$

The loss  $\mathcal{L}_{percep}(x_i, \mathbf{z}_i; \theta)$ , defined in (1), measures the reconstruction loss between  $G_\theta(\mathbf{z}_i)$  and  $x_i$ . We note that while in the original GLO the Laplacian pyramid loss is used instead of  $\mathcal{L}_{percep}$ , the minimization of  $\mathcal{L}_{percep}$  appears to yield more realistic results (Hoshen & Malik, 2018).

**Adding a Classifier.** Possibly the main weakness of using GLO as a generative model is the relative low quality of images generated when sampling new points in the latent space  $Z$ . The problem lies in the sparsity of the learned set  $\{\mathbf{z}_i\}_{i=1}^n$ , which lacks structure since each  $\mathbf{z}_i$  is trained independently. In order to decrease the intra-class distances and increase the inter-class distances in the latent space representation, we propose the conditional model cGLO. In this model, generator  $G_\theta$  is augmented by a weak classifier  $f_\phi$ , which is trained to classify the labeled data. When the

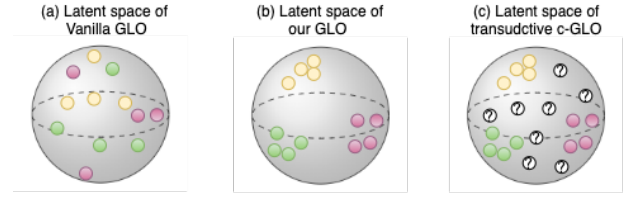


Figure 2. Illustration of the latent space  $Z$  in our method vs. vanilla GLO. (a) Vanilla GLO: vectors  $\mathbf{z}_i \in Z$  do not have semantic meaning in  $Z$ . (b) Our method: vectors from the same class are grouped. (c) Our method in transductive mode. Notations: filled colored circles represent different labeled datapoints, where color corresponds to class identity. Black circles with the symbol “?” represent unlabeled datapoints.

label of  $x_i$  is known,  $\mathcal{L}_{percep}$  in (2) is replaced by  $\mathcal{L}_{percep} + \mathcal{L}_{ce}$ , where  $\mathcal{L}_{ce}$  is the cross-entropy loss of classifier  $f_\phi$ .

**Sampling the Latent Space.** Generating images based on randomly sampling the latent space, even when restricted to the immediate vicinity of  $\{\mathbf{z}_i\}_{i=1}^n$ , still produces low quality somewhat meaningless images. Therefore, instead of randomly sampling  $Z$ , we generate new image codes by interpolating between the known latent vectors  $\{\mathbf{z}_i\}_{i=1}^n$ . Since the latent space  $Z$  is a hyper-sphere, we employ to this end *spherical linear interpolation (slerp)* (Shoemake, 1985), which is defined as follows:

$$slerp(q_1, q_2; t) = q_1 \frac{\sin((1-t)\vartheta)}{\sin \vartheta} + q_2 \frac{\sin t\vartheta}{\sin \vartheta} \quad (3)$$

Above  $t \in [0, 1]$ , and  $\vartheta$  is the angle between  $q_1$  and  $q_2$ , computed as  $\vartheta = \cos^{-1}(q_1 \cdot q_2)$ .

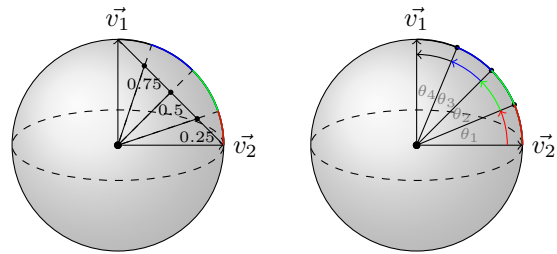


Figure 3. *Slerp* vs. *lerp*. Left side: linear interpolation between  $\vec{v}_1$  and  $\vec{v}_2$  with  $t \in [0.25, 0.5, 0.75]$ . Right side: spherical interpolation. Note that both the length and arc length of the interpolated vectors are equal in *slerp* but unequal in *lerp*.

As shown in Fig. 3, in *slerp* interpolation follows the great circle path on an  $d$ -dimensional hyper-sphere (with elevation changes) between two points  $\mathbf{z}_i$  and  $\mathbf{z}_j$ . This technique has shown promising results in the context of both VAE and GAN generative models and with both uniform and Gaussian priors (White, 2016).

Why *slerp*? Linear interpolation (*lerp*) is the simplest method to traverse the latent space manifold between two known locations. Often it is used to show inartistic learned features which capture the semantics of the dataset (e.g., [karpathy, 2014](#); [Krizhevsky et al., 2012b](#)). However, [Arvanitidis et al. \(2017\)](#) noted that linear interpolation in the latent space is often inappropriate, since the latent spaces of most generative models are embedded in high dimensional spaces (over 50 dimensions). In such a space, linear interpolation traverses locations that are extremely unlikely given the prior, whether Gaussian or uniform.

**Noise concatenation.** Training from a small sample is more susceptible than ever to random perturbations in the data. To increase training robustness, we concatenate noise to the latent vector such that the input to the generator  $G_\theta$  is  $[\mathbf{z}_i, \varepsilon]$   $\varepsilon \sim N(0, \sigma I)$ , see Fig. 1. In effect, this introduces randomness into the training via the batch normalization layers ([Ioffe & Szegedy, 2015](#)).

**Transductive learning.** The setting of transductive learning was introduced by [Vapnik \(1998\)](#). Like semi-supervised learning it aims to exploit unlabeled data, using the unlabeled test set to improve the test set classification.

Specifically, the learning task is defined on a given set of  $\ell$  training points

$$\{(\mathbf{x}_1, y_1), (\mathbf{x}_2, y_2), \dots, (\mathbf{x}_\ell, y_\ell)\}, \mathbf{x}_i \in \mathbb{R}^d, y_i \in \{-1, 1\}$$

and a sequence of  $k$  test vectors  $\{\mathbf{x}_{\ell+1}, \dots, \mathbf{x}_{\ell+k}\}$ . The goal of the learner is to find among an admissible set of binary vectors the one that classifies the test vectors as accurately as possible. We assume that the set of vectors  $\{\mathbf{x}_{\ell+1}, \dots, \mathbf{x}_{\ell+k}\}$  and their corresponding true labels is an i.i.d sample drawn according to the same unknown distribution  $P(\mathbf{x})$  and  $P(y|\mathbf{x})$ . Basically, the core idea in transductive learning is to leverage the implicit information in the instances whose output is required ( $\mathbf{x}_{\ell+1}, \dots, \mathbf{x}_{\ell+k}$ ), in order to improve their classification.

In the same spirit as the classical setting of transductive learning, we may use the test data in order to train the generator of the model to reconstruct the test points while optimizing their reconstruction loss (2), see Fig. 3.2.

## 4. Evaluation Methodology

### 4.1. Datasets

We evaluate our method on two standard benchmarks for image classification. The first is CIFAR-100 ([Krizhevsky et al.](#)), which includes 50,000  $32 \times 32$  color images, with 100 classes and 500 images per class. The relative small size of the images allows us to perform an exhaustive ablation study on this dataset as described in Section 5. The second

dataset is CUB-200 ([Wah et al., 2011](#)), which includes high resolution fine-grained images of 200 species of birds, with only 30 images per class. This makes this dataset a more appropriate test bed for a method which addresses the small sample problem.

### 4.2. Experimental Protocol

For each benchmark we defined a small-sample task by sub-sampling the original training set of the corresponding dataset. To allow for comparison with other methods, the subset splits were adapted from ([Barz & Denzler, 2019](#)). As classification engine we used, unless otherwise noted, the *WideResNet-28* model ([Zagoruyko & Komodakis, 2016](#)) for CIFAR-100, and the Resnet50 model ([He et al., 2016](#)) for CUB-200. Baseline results were obtained by training the corresponding model using the training set with only standard data augmentation.

When using our method, we augmented the training set using cGLO. Specifically, we start by sampling a mini-batch from the training data in each SGD optimization step. Each example  $x_i$  in the mini-batch is used for training with probability 0.5. Otherwise (with probability 0.5) it is replaced by a new image obtained by sampling the latent space  $G(\text{slerp}(\mathbf{z}_i, \mathbf{z}_j, t))$ .  $\mathbf{z}_j$  is the latent representation of some example from the same class  $c$  as  $x_i$ , sampled uniformly from the latent codes of all remaining examples in class  $c$ . The *slerp* interpolation factor is sampled uniformly from the set  $[0.1, 0.2, 0.3, 0.4]$ .

We compared our results with state-of-the-art methods which are suitable for the small sample domain, using as much as possible public-domain code. Thus we compared sample augmentation with cGLO to image augmentation with Cutout ([DeVries & Taylor, 2017b](#)), Random Erase ([Zhong et al., 2017](#)) and MixMatch ([Berthelot et al., 2019](#)). In each case we repeated the same procedure as described above, replacing the generation of a new image using cGLO by an image obtained from the corresponding augmented set of images. We also evaluated the method described in ([Barz & Denzler, 2019](#)), which was explicitly designed to handle small sample, using code provided by the authors.

### 4.3. Implementation Details

We used SGD optimization with learning rate 0.1 for CIFAR-100 and 0.001 for CUB-200, with batch size of 128 and 16 respectively. In all the experiments we used the standard categorical cross-entropy loss function when training the weak classifier  $f\phi$ . (We note in passing that using a strong classifier decreased the quality of the generated images and harmed the final performance.) Images from the CUB-200 dataset were resized to 256 pixels wide in their smaller side, and then randomly cropped to  $224 \times 224$  pixels. As stated above, in all the experiments (including baseline) we

## Learning from Small Data Through Sampling a Conditional GLO Model

SAMPLES/CLASS	BASELINE	CGLO	MIXMATCH	CUTOUT	RANDOM ERASE	BARZ & DENZLER
10	22.89 ± 0.09	<b>28.55 ± 0.40</b>	24.8	23.43 ± 0.24	23.26 ± 0.27	23.01 (22)
25	38.39 ± 0.18	<b>43.84 ± 0.25</b>	40.17	39.11 ± 0.59	37.45 ± 0.15	28.05 (35)
50	47.82 ± 0.11	<b>52.95 ± 0.20</b>	49.87	52.11 ± 0.28	50.5 ± 0.41	44.55 (48)
100	61.37 ± 0.13	64.27 ± 0.04	59.03	<b>64.49 ± 0.10</b>	64.03 ± 0.22	55.99 (58)

Table 1. Comparison of Top-1 Accuracy (including STE) for CIFAR-100 using WideResnet-28, with a different number of training examples per class. The methods used for comparison are described in the text below, where caveats regarding the results reported in the last column are also discussed. Best results are marked in bold.

SAMPLES/CLASS	BASELINE	CGLO	MIXMATCH	CUTOUT	RANDOM ERASE	BARZ & DENZLER
5	50.79 ± 0.19	<b>51.52 ± 0.21</b>	15.01	50.63 ± 0.31	48.90 ± 0.45	17.80 (35)
10	64.11 ± 0.22	<b>65.13 ± 0.12</b>	36.02	64.33 ± 0.02	63.72 ± 0.20	34.23 (60)
20	69.11 ± 0.55	<b>74.16 ± 0.17</b>	60.57	68.47 ± 0.20	66.14 ± 0.23	52.00 (76)
30	75.15 ± 0.10	<b>77.75 ± 0.20</b>	70.41	74.97 ± 0.34	73.74 ± 0.34	62.25 (82.5)

Table 2. Comparison of Top-1 Accuracy (including STE) for CUB-200 using ResNet-50, with a different number of training examples per class. The methods used for comparison are described in the text below, including some caveats. Best results are marked in bold.

adopted the standard transformations of random horizontal flipping and random crop for data augmentation.

In all cases the latent space  $Z$  was the unit sphere in  $\mathbb{R}^{128}$ . For the generator we used a standard off-the-shelf DCGAN architecture (Radford et al., 2015). More modern GAN architecture can be readily used instead and improve the reconstruction quality. However, it is worth noting that our method can improve the SOTA while using a relatively simple GAN architecture. We trained the model on  $2 \times$  Tesla P100 GPUs for 200 epochs; every epoch took around 40 seconds on CIFAR-100 and 3 minutes on CUB-200.

To achieve uniformity we oversampled the training set in proportion to the size of the training set. For example, with 50 samples per class in CIFAR-100 we trained the model  $\times 10$  iterations. Standard errors (STE) were obtained from 3 runs with different seeds in all study cases except for MixMatch, where a single result is reported since each MixMatch run took a very long time.

## 5. Results

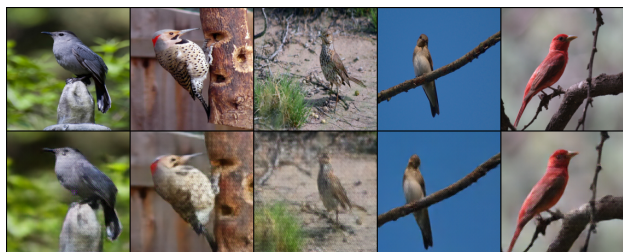


Figure 4. CUB-200 Reconstruction results: upper row shows the original image, second row shows the corresponding reconstructed image. cGLO was trained only on 10 examples per class.

The results of our empirical study are summarized in Table 1



Figure 5. CIFAR-100 with 10 samples per class. Each row shows 7 new images generated based on smooth interpolation in the latent space between 2 reconstructed images.

for CIFAR-100, and Table 2 for CUB-200. We used small sample partitions, with 10 to 100 labeled images per class in CIFAR-100, and 5 to 30 labeled images per class in CUB-200. We compared our model to three different methods of data augmentation and one small sample method.

Fig. 4 illustrates the quality of the reconstruction when using cGLO, showing a relatively precise though somewhat blurred reconstruction. Fig. 5 illustrates the kind of synthetic images we get while relying on a very small sample. Note that since the purpose of generating new images is to boost

Model	Top 1 Acc.	Top 5 Acc.
cGLO	43.84 ± 0.25	67.77±0.18
Baseline	38.39±0.18	67.77±0.18
no classifier	41.57 ± 0.54	69.55±0.11
no Noise	43.31±0.02	70.05±0.02
<i>lerp</i>	43.01±0.06	70.51±0.03
Transductive	44.39± 0.12	71.28±0.09

Table 3. Ablation Study: Top 1 and Top 5 accuracy is calculated based on the architectural variants described Section 5.1.

classification from small sample, low image quality does not preclude their usefulness for the task.

The two augmentation methods used in our comparisons, Random Erasing (Zhong et al., 2017) and Cutout (DeVries & Taylor, 2017b), achieve a relatively good performance; with CIFAR-100 and a 100 samples per class, Cutout achieves the highest accuracy (similar to cGLO) in our experiments. Nevertheless, in all the other small sample cases we have studied cGLO significantly outperforms these methods.

MixMatch (Berthelot et al., 2019) is a new technique that achieves state-of-the-art results on multiple datasets in a semi-supervised setting. In the supervised small sample regime, this method does not perform very well as can be seen in Tables 1 and 2, but see Section 5.4. Possibly, the blending of images in pixel space, which is intended to provide some means of regularization, is only effective when enough training data is available. Otherwise, it feeds noisy examples to the model and makes it harder to generalize.

Barz & Denzler (2019) describe a distance based method which is designed to handle the small sample challenge, among other things. The results, when using the code published by the authors in our experimental design, are shown in the last column of Tables 1 and 2. Admittedly, we were not able to reproduce their published results. We therefore show in round brackets our best estimate of their original results, which were only reported in a pictorial format<sup>1</sup>

### 5.1. Ablation Study

In this section, we review and evaluate different design choices used in the architecture and the approach proposed in this paper. In this ablation study we used CIFAR-100 with 25 labeled training examples per class. The results are summarized in Table 3.

More specifically, we see in Table 3 the effect of omitting different components of cGLO, including classifier  $f_\phi$ , noise concatenation, and replacing *slerp* by vanilla linear interpo-

<sup>1</sup>These experiments used Resnet-110 for CIFAR-100 rather than the WideResNet-28 model used here, and Resnet-50 for CUB-200 as in our experiments.

Model	Top 1 Acc.	Top 5 Acc.
Latent classifier	43.08 ± 0.06	70.22±0.05
Hypercube init	44.21± 0.61	70.89 ±0.46
ResNet init	42.95±0.22	70.10 ±0.13
Additive noise	41.02±0.43	68.10±0.11
Cosine Loss	41.01± 0.27	68.45±0.31

Table 4. Top 1 and Top 5 accuracy of additional design choices as explained in the text.

lation. We note that when omitting classifier  $f_\phi$ , the reconstruction loss achieves a better score, but the augmentation fails to generate ‘good’ examples to improve classification. The ‘Baseline’ case shows the results of training without sampling additional images. ‘Transductive’ shows the added benefit obtained from including the unlabeled test set in the training of generator  $G_\theta$ .

### 5.2. Additional Design Choices

In this section we describe a few alternative design choices that proved less effective, as summarized in Table 4.

**Latent Classifier.** One can optimize the discriminative loss  $\mathcal{L}_{CE}$  directly in the latent space using  $(\mathbf{z}_i, y_i)$  instead of the image space  $(G(\mathbf{z}_i), y_i)$ . Here we used a 3 layer fully connected network with inter-layer ReLU activation.

**Z Initialization.** We investigated different ways to initialize the latent space mappings while exploiting some prior knowledge we have on the data, including: **i)** Hypercube vertices: every class is initialized in the vicinity of a different vertex of the hypercube in  $\mathbb{R}^{128}$ . **ii)** ResNet: each image is assigned the corresponding activation in the penultimate layer of a pre-trained ResNet model.

**Additive Noise.** cGLO relies on the concatenation of noise to the latent space representation. To investigate the contribution of this mechanism, and following (Lehtinen et al., 2018), we explored a simpler alternative, where random noise  $\varepsilon \sim \mathcal{N}(0, \sigma I)$  is sampled i.i.d and added to  $\mathbf{z}_i$  before calculating the loss (2). The goal is to obtain a better representation of the image manifold by learning the  $\varepsilon$  ball around every example both in the latent space and the image space. However, as shown in Table 4, this approach leads to performance degradation in the final classification.

**Cosine Loss.** It is argued in (Barz & Denzler, 2019) that the cosine loss is a better optimization function for the small sample regime. In our experimental setup the cross-entropy classification loss provided better results, see Table 4.

Method	supervised only	1000 unlabeled	35k unlabeled
Baseline	$38.39 \pm 0.18$	-	-
MixMatch	40.17	42.39	50.34
cGLO	$43.84 \pm 0.25$	$44.52 \pm 0.12$	$44.73 \pm 0.07$

Table 5. Semisupervised scenario: Top-1 Accuracy of MixMatch vs cGLO when shown 25 labeled examples per class and a varying number of unlabeled examples, where each case corresponds to a different column.

### 5.3. Relation to Classical Augmentations

Next, we investigate the relationship between new images generated by our method and images generated by methods using classical augmentation techniques. To this end we adopt AutoAugment (Cubuk et al., 2018), a method designed to find a proxy for the optimal set of classical transformations to augment images in CIFAR-100, searching through 16 types of color-based and geometric base transformations. The case studied here is CIFAR100 with 50 labeled examples per class, and with transductive learning (similar results are obtained without transductive learning).

When using the two methods - AutoAugment and cGLO - in conjunction, each method seems to provide an independent contribution as shown in Table 6. From this we conclude that the contribution of cGLO goes beyond the contribution of augmentation by classical image transformation. Note that AutoAugment is trained on the entire training set of CIFAR-100 so the direct comparison of our method to this policy is not applicable.

AutoAu.	cGLO	Top-1 Accuracy	Top-5 Accuracy
		$50.37 \pm 0.05$	$75.61 \pm 0.01$
	✓	$53.35 \pm 0.23$	$77.60 \pm 0.12$
✓		$53.80 \pm 0.10$	$79.18 \pm 0.13$
✓	✓	$56.31 \pm 0.02$	$80.66 \pm 0.04$

Table 6. Top-1 and Top-5 accuracy when augmenting a small dataset by cGLO alone (second row), AutoAugment alone (third row), or both (fourth row). Note that each method boosts performance on its own, while when used in conjunction additional performance boost is seen.

### 5.4. Using Unlabeled Data

While in the fully supervised scenario cGLO outperforms MixMatch as shown in Tables 1 and 2, MixMatch performs better when given access to unlabeled data, and eventually it outperforms cGLO as shown in Table 5. cGLO can also use unlabeled data to boost the training of the generator  $G_\theta$ , but as shown in Table 5, clearly MixMatch benefits from unlabeled data more considerably. We note that cGLO can benefit from using the test data during training following the transductive learning procedure, which is another way

of using unlabeled data to boost training.

## 6. Summary and Discussion

In this work we revisited the problem of learning from small sample. We developed a deep generative model, conditional GLO (cGLO), which can be effectively trained to generate examples when seeing only a small sample of data. New examples are synthesized by interpolating between the latent vectors of known examples. When using small sample scenarios generated from the CIFAR-100 and CUB-200 benchmarks, we show that our method improves classification over the baseline and over a number of alternative methods. Thus our method defines the state of the art in small sample image classification.

Our generative model is based on latent space optimization. Latent optimization does not involve an encoder like some other generative methods (such as the Variational Auto Encoder). In particular, this implies that the number of variables grows linearly with the number of data samples. Contrary to GAN, latent optimization learns every latent representation separately, and therefore it does not require much data in order to achieve decent reconstruction results as demonstrated in Fig. 4.

The optimization of each representation vector separately also implies that the dimensions of the latent space do not correspond to semantic features of the data. To address this weakness and inject some semantic structure into the latent space representation, we added a classifier to the latent optimization training process. Unlike GANs, the classifier is not trained in an adversarial fashion. Rather, we use the classification loss  $\mathcal{L}_{CE}$  over the reconstructed examples  $G_\theta(\mathbf{z}_i)$  to induce semantic relations into the latent space, and allow for better sampling and new image generation (see Fig. 2).

The unique aforementioned properties of our model allow it to improve the training efficacy of deep classifiers in the small sample regime. In this regime, the classifier only sees a small number of labeled examples from each class. Two complementary approaches, which can be used in conjunction with our method, may benefit from unlabeled data in a semi-supervised manner, or unrelated labeled datasets which can be used for transfer learning.



## References

- Antoniou, A., Storkey, A., and Edwards, H. Augmenting image classifiers using data augmentation generative adversarial networks. In *International Conference on Artificial Neural Networks*, pp. 594–603. Springer, 2018.
- Arvanitidis, G., Hansen, L. K., and Hauberg, S. Latent space oddity: on the curvature of deep generative models, 2017.
- Baird, H. S. Document image defect models and their uses. *Proceedings of 2nd International Conference on Document Analysis and Recognition (ICDAR '93)*, pp. 62–67, 1993.
- Barz, B. and Denzler, J. Deep learning on small datasets without pre-training using cosine loss. *CoRR*, abs/1901.09054, 2019. URL <http://arxiv.org/abs/1901.09054>.
- Baxter, J. A bayesian/information theoretic model of learning to learn via multiple task sampling. In *Machine Learning*, pp. 7–39, 1997.
- Berthelot, D., Carlini, N., Goodfellow, I., Papernot, N., Oliver, A., and Raffel, C. Mixmatch: A holistic approach to semi-supervised learning. *arXiv preprint arXiv:1905.02249*, 2019.
- Bojanowski, P., Joulin, A., Lopez-Pas, D., and Szlam, A. Optimizing the latent space of generative networks. In Dy, J. and Krause, A. (eds.), *Proceedings of the 35th International Conference on Machine Learning*, volume 80 of *Proceedings of Machine Learning Research*, pp. 600–609, Stockholm, Sweden, 10–15 Jul 2018. PMLR. URL <http://proceedings.mlr.press/v80/bojanowski18a.html>.
- Brock, A., Donahue, J., and Simonyan, K. Large scale gan training for high fidelity natural image synthesis. *arXiv preprint arXiv:1809.11096*, 2018.
- Chawla, N. V., Bowyer, K. W., Hall, L. O., and Kegelmeyer, W. P. Smote: synthetic minority over-sampling technique. *Journal of artificial intelligence research*, 16:321–357, 2002.
- Cubuk, E. D., Zoph, B., Mané, D., Vasudevan, V., and Le, Q. V. Autoaugment: Learning augmentation policies from data. *CoRR*, abs/1805.09501, 2018.
- DeVries, T. and Taylor, G. W. Dataset augmentation in feature space. *arXiv preprint arXiv:1702.05538*, 2017a.
- DeVries, T. and Taylor, G. W. Improved regularization of convolutional neural networks with cutout. *arXiv preprint arXiv:1708.04552*, 2017b.
- Fadaee, M., Bisazza, A., and Monz, C. Data augmentation for low-resource neural machine translation. *arXiv preprint arXiv:1705.00440*, 2017.
- Fei-Fei, L., Fergus, R., and Perona, P. Learning generative visual models from few training examples: An incremental bayesian approach tested on 101 object categories. 2004.
- Goodfellow, I. J. Nips 2016 tutorial: Generative adversarial networks. *ArXiv*, abs/1701.00160, 2017.
- Hataya, R., Zdenek, J., Yoshizoe, K., and Nakayama, H. Faster autoaugment: Learning augmentation strategies using backpropagation. *arXiv preprint arXiv:1911.06987*, 2019.
- He, K., Zhang, X., Ren, S., and Sun, J. Deep residual learning for image recognition. In *Proceedings of the IEEE conference on computer vision and pattern recognition*, pp. 770–778, 2016.
- Hertz, T., Hillel, A. B., and Weinshall, D. Learning a kernel function for classification with small training samples. In *Proceedings of the 23rd international conference on Machine learning*, pp. 401–408, 2006.
- Hoshen, Y. and Malik, J. Non-adversarial image synthesis with generative latent nearest neighbors. *CoRR*, abs/1812.08985, 2018. URL <http://arxiv.org/abs/1812.08985>.
- Ioffe, S. and Szegedy, C. Batch normalization: Accelerating deep network training by reducing internal covariate shift. *arXiv preprint arXiv:1502.03167*, 2015.
- Johnson, J., Alahi, A., and Fei-Fei, L. Perceptual losses for real-time style transfer and super-resolution. In *European conference on computer vision*, pp. 694–711. Springer, 2016.
- karpathy, A. t-sne visualization of cnn codes, 2014. URL <https://cs.stanford.edu/people/karpathy/cnnembed/>.
- Karras, T., Laine, S., and Aila, T. A style-based generator architecture for generative adversarial networks. In *Proceedings of the IEEE Conference on Computer Vision and Pattern Recognition*, pp. 4401–4410, 2019.
- Kobayashi, S. Contextual augmentation: Data augmentation by words with paradigmatic relations. In *Proceedings of the 2018 Conference of the North American Chapter of the Association for Computational Linguistics: Human Language Technologies, Volume 2 (Short Papers)*, pp. 452–457, New Orleans, Louisiana, June 2018. Association for Computational Linguistics. doi: 10.18653/v1/N18-2072. URL <https://www.aclweb.org/anthology/N18-2072>.

- Krizhevsky, A., Nair, V., and Hinton, G. Cifar-100 (canadian institute for advanced research). URL <http://www.cs.toronto.edu/~kriz/cifar.html>.
- Krizhevsky, A., Sutskever, I., and Hinton, G. E. Imagenet classification with deep convolutional neural networks. In *NIPS*, 2012a.
- Krizhevsky, A., Sutskever, I., and Hinton, G. E. Imagenet classification with deep convolutional neural networks. In Pereira, F., Burges, C. J. C., Bottou, L., and Weinberger, K. Q. (eds.), *Advances in Neural Information Processing Systems 25*, pp. 1097–1105. Curran Associates, Inc., 2012b. URL <http://papers.nips.cc/paper/4824-imagenet-classification-with-deep-convolutional-neural-networks.pdf>.
- Lehtinen, J., Munkberg, J., Hasselgren, J., Laine, S., Karras, T., Aittala, M., and Aila, T. Noise2noise: Learning image restoration without clean data. *arXiv preprint arXiv:1803.04189*, 2018.
- Lemley, J., Bazrafkan, S., and Corcoran, P. Smart augmentation learning an optimal data augmentation strategy. *Ieee Access*, 5:5858–5869, 2017.
- Li, W., Wang, L., Xu, J., Huo, J., Gao, Y., and Luo, J. Revisiting local descriptor based image-to-class measure for few-shot learning. In *Proceedings of the IEEE Conference on Computer Vision and Pattern Recognition*, pp. 7260–7268, 2019.
- Lim, S., Kim, I., Kim, T., Kim, C., and Kim, S. Fast autoaugment. In *NeurIPS*, 2019.
- Liu, X., Zou, Y., Kong, L., Diao, Z., Yan, J., Wang, J., Li, S., Jia, P., and You, J. Data augmentation via latent space interpolation for image classification. In *2018 24th International Conference on Pattern Recognition (ICPR)*, pp. 728–733. IEEE, 2018.
- Odena, A. Semi-supervised learning with generative adversarial networks. *arXiv preprint arXiv:1606.01583*, 2016.
- Park, D. S., Chan, W., Zhang, Y., Chiu, C.-C., Zoph, B., Cubuk, E. D., and Le, Q. V. Specaugment: A simple data augmentation method for automatic speech recognition. *arXiv preprint arXiv:1904.08779*, 2019.
- Radford, A., Metz, L., and Chintala, S. Unsupervised representation learning with deep convolutional generative adversarial networks. *arXiv preprint arXiv:1511.06434*, 2015.
- Schwartz, E., Karlinsky, L., Shtok, J., Harary, S., Marder, M., Kumar, A., Feris, R., Giryas, R., and Bronstein, A. Delta-encoder: an effective sample synthesis method for few-shot object recognition. In *Advances in Neural Information Processing Systems*, pp. 2845–2855, 2018.
- Shoemake, K. Animating rotation with quaternion curves. *SIGGRAPH Comput. Graph.*, 19(3):245–254, July 1985. ISSN 0097-8930. doi: 10.1145/325165.325242. URL <http://doi.acm.org/10.1145/325165.325242>.
- Tanner, M. A. and Wong, W. H. The calculation of posterior distributions by data augmentation. 1987.
- Thrun, S. and Pratt, L. Y. Learning to learn. In *Springer US*, 1998.
- Vapnik, V. V. Statistical learning theory, 1998.
- Wah, C., Branson, S., Welinder, P., Perona, P., and Belongie, S. The Caltech-UCSD Birds-200-2011 Dataset. Technical Report CNS-TR-2011-001, California Institute of Technology, 2011.
- Wang, X., Pham, H., Dai, Z., and Neubig, G. SwitchOut: an efficient data augmentation algorithm for neural machine translation. In *Proceedings of the 2018 Conference on Empirical Methods in Natural Language Processing*, pp. 856–861, Brussels, Belgium, October–November 2018. Association for Computational Linguistics. doi: 10.18653/v1/D18-1100. URL <https://www.aclweb.org/anthology/D18-1100>.
- White, T. Sampling generative networks: Notes on a few effective techniques. *CoRR*, abs/1609.04468, 2016. URL <http://arxiv.org/abs/1609.04468>.
- Zagoruyko, S. and Komodakis, N. Wide residual networks. *arXiv preprint arXiv:1605.07146*, 2016.
- Zhang, H., Cisse, M., Dauphin, Y. N., and Lopez-Paz, D. mixup: Beyond empirical risk minimization. *arXiv preprint arXiv:1710.09412*, 2017.
- Zhang, X., Zhao, J., and LeCun, Y. Character-level convolutional networks for text classification. In *Advances in neural information processing systems*, pp. 649–657, 2015.
- Zhang, X., Wang, Z., Liu, D., and Ling, Q. Dada: Deep adversarial data augmentation for extremely low data regime classification. In *ICASSP 2019-2019 IEEE International Conference on Acoustics, Speech and Signal Processing (ICASSP)*, pp. 2807–2811. IEEE, 2019.
- Zhong, Z., Zheng, L., Kang, G., Li, S., and Yang, Y. Random erasing data augmentation. *arXiv preprint arXiv:1708.04896*, 2017.